Supplementary Information

Perylene Tetracarboxylate Dye Based Colorimetric and Fluorometric Sensor for ppb-Level Fluoride Detection in Water

Bikash Chandra Musahary,[a] Debajit Bora[a], Chayanika Goswami[a], Rituraj Das[b] and Sanjeev Pran Mahanta *[a]

[a]Department of Chemical Sciences, Tezpur University, Tezpur, Assam 784028, India.

[b]Department of Chemistry, Morigaon College, Morigaon, Assam 782105, India.

[*]**Corresponding author, E-mail**:-spm@tezu.ernet.in, samahanta@gmail.com

Table of contents

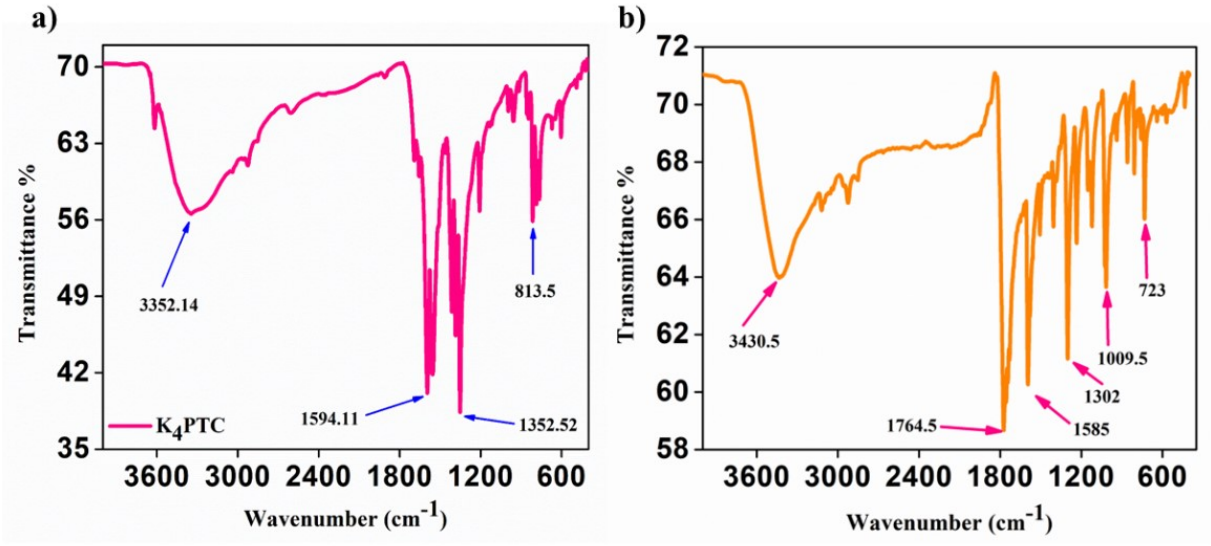

Figure S1: FT-IR spectrum of a) K_4PTC and b) isolated complex of Al^{3+} and PTC^{4-}.

[Fig S1 a): The absorption bands at 1594 cm^{-1} and 1352.5 cm^{-1} are attributed to the asymmetric and symmetric vibrations, respectively, of COO^- in **K_4PTC**, b) The absorption peak at 1764.5 cm^{-1} is indicative of asymmetric vibration of COO^- group of the isolated complex of Al^{3+} and PTC^{4-}. The peaks at 1585 cm^{-1} and 723 cm^{-1} represent the stretching frequencies of C-O and Al-O bonds, respectively.]

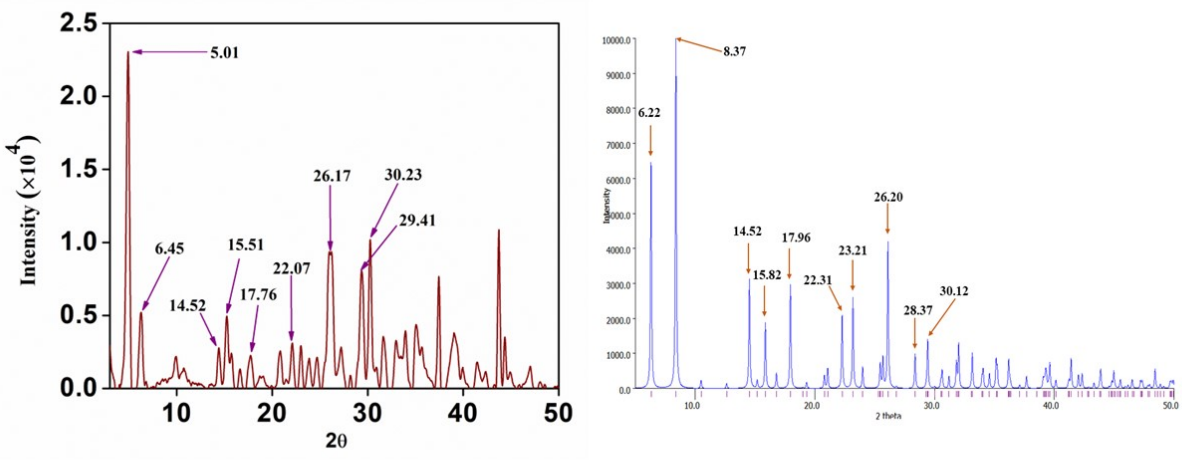

Figure S2: Powder X-ray diffraction pattern of K4PTC MOF and comparison with the PXRD of the reported one (CCDC Number: 1509483).

K_4PTC (This work)	PXRD of K_4PTC MOF simulated from the reported crystal data CCDC number: 1509483
14.52°	14.52°
15.51°	15.58°
17.76°	17.96°
26.17°	26.20°
29.41°	28.32°
30.23°	30.12°

Table S1: Comparison of the PXRD 2Θ values of the peaks of the K_4PTC synthesized with the PXRD simulated from the cif file of the reported data (Ref: Ref: J. M. Seco, E. San Sebastián, J. Cepeda, B. Biel, A. Salinas-Castillo, B. Fernández, D. P. Morales, M. Bobinger, S. Gómez-Ruiz, F. C. Loghin, A. Rivadeneyra, A. Rodríguez-Diéguez, Sci. Rep., 2018, 8, 14414).

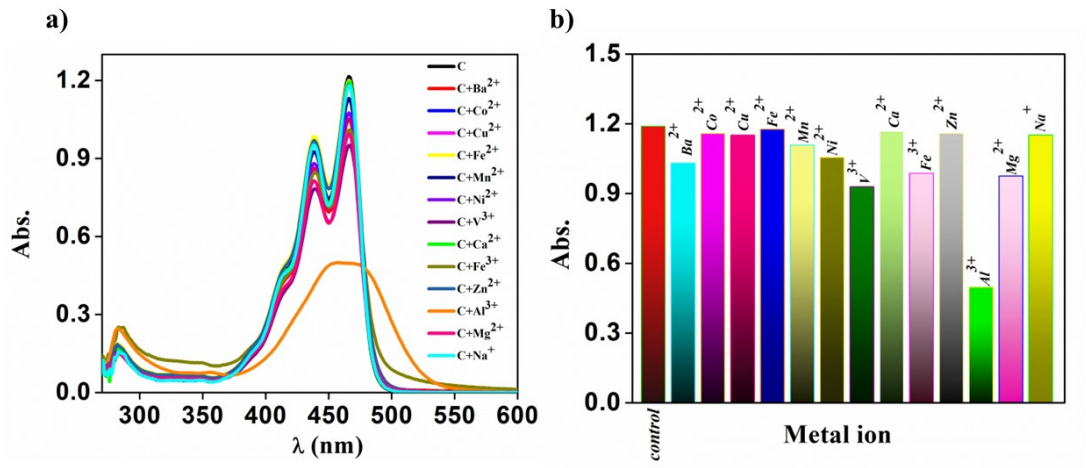

Figure S3: a) UV−Vis absorption spectra of **K_4PTC** [1.6 × 10^{-4} M] solution in water upon addition of 5 equivalent of various metal ions [1 × 10^{-2} M] in water ($BaCl_2$, $CoCl_2$, $CuCl_2$, $FeCl_2$, $MnCl_2$, $NiCl_2$, VCl_3, $CaCl_2$, $FeCl_3$, $ZnCl_2$, $AlCl_3$, $MgCl_2$, NaCl) (C: **K_4PTC**), b) Bar representation of the change in absorbance at 480 nm, where ***Control, C*= K_4PTC..**

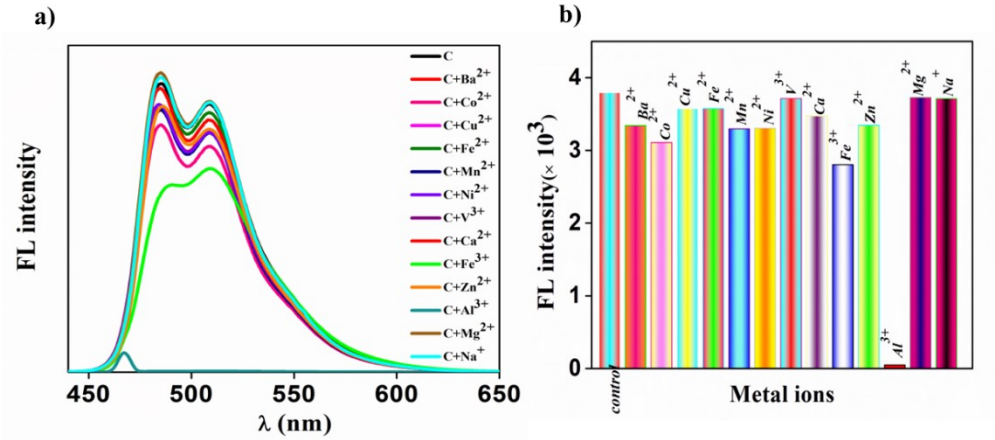

Figure S4: a) Emission spectra of **K_4PTC** [1 × 10^{-3} M] in water upon addition of 5 equivalent of various metal ions [1 × 10^{-3} M] in water ($BaCl_2$, $CoCl_2$, $CuCl_2$, $FeCl_2$, $MnCl_2$, $NiCl_2$, VCl_3, $CaCl_2$, $FeCl_3$, $ZnCl_2$, $AlCl_3$, $MgCl_2$, NaCl) (C: **K_4PTC**), b) Bar representation of the change in intensity of the emission at 550 nm, where ***Control, C*= K_4PTC.**

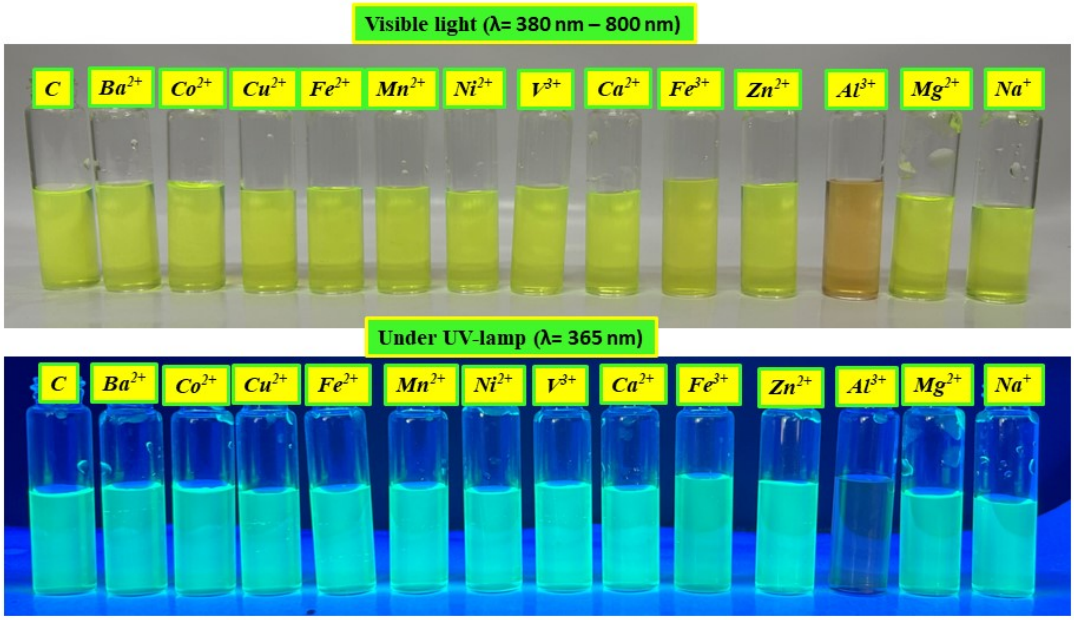

Figure S5: Change in colour of **K_4PTC solution in water** upon addition of 5 equivalents of various metal ions under normal light and UV lamp.

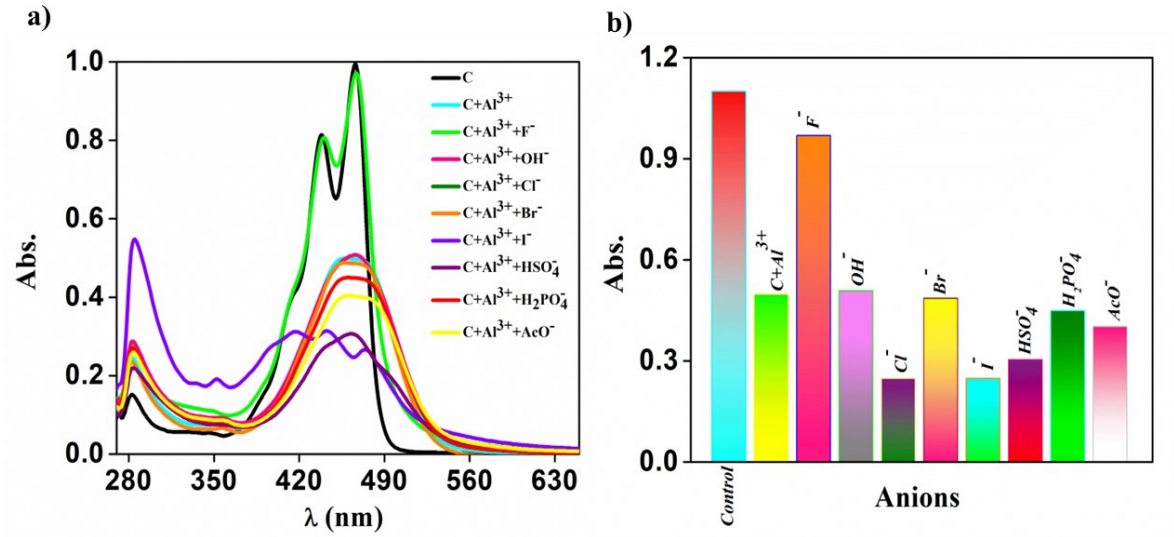

Figure S6: a) UV−Vis absorption spectra of **K_4PTC** [1×10^{-3} M] solution in water upon addition of different anions [1×10^{-2} M] in presence of Al^{3+} [1×10^{-2} M] ion (C: **K_4PTC**), b) Bar representation of the change in absorbance at 465 nm, where ***Control, C*** = **K_4PTC.**

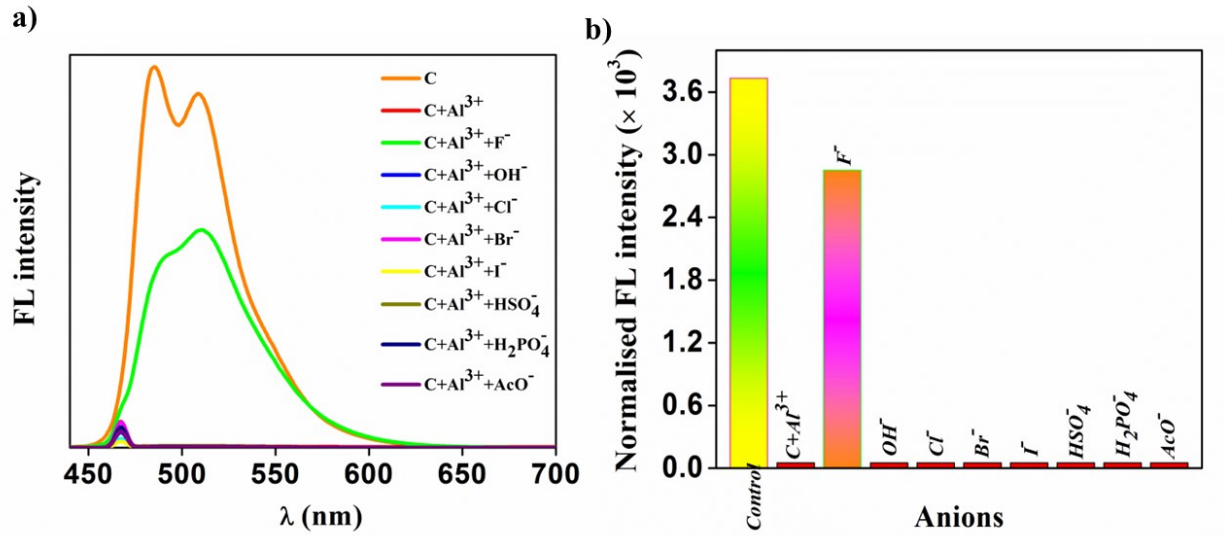

Figure S7: a) Emission spectra of **K_4PTC** [1 × 10^{-3} M] upon addition of various anions [1 × 10^{-3} M], in presence of Al^{3+} [1 × 10^{-3} M], λ_{exc}= 465 nm) (C: **K_4PTC**); b) Bar representation of the change in intensity of the emission at 550 nm, where ***Control, C*** = **K_4PTC.**

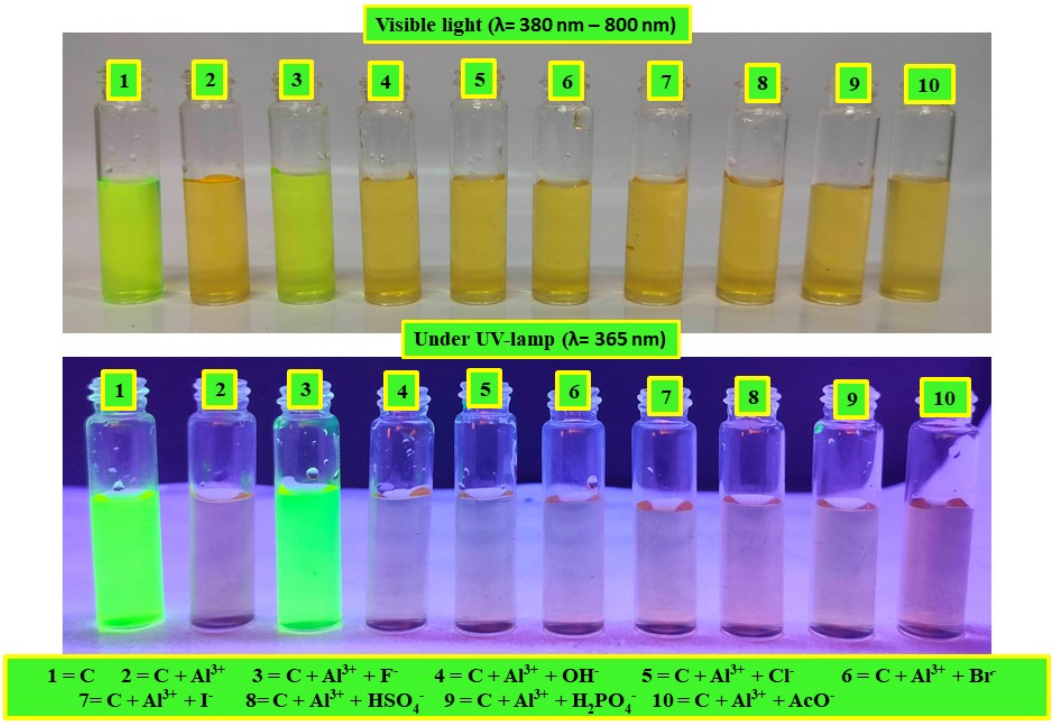

Figure S8: Change in colour of the K_4PTC solution in water upon addition of different anions in presence of Al^{3+} ion in normal light and UV lamp.

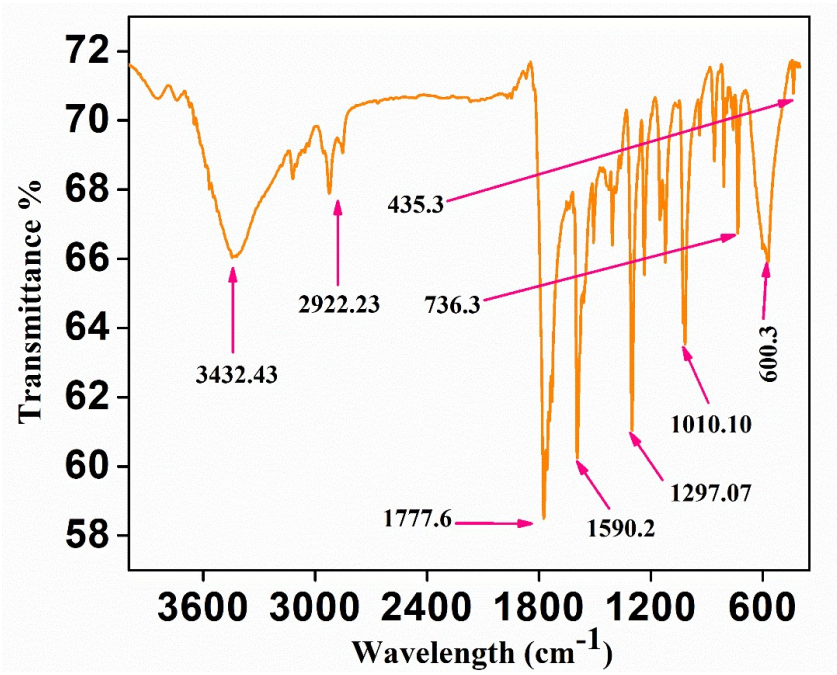

Figure S9: FT-IR spectrum of K_4PTC upon addition of NaF in presence of Al^{3+}. (The peak at 600 cm^{-1} represents the F-Al-F stretching indicating the formation of AlF_3.)

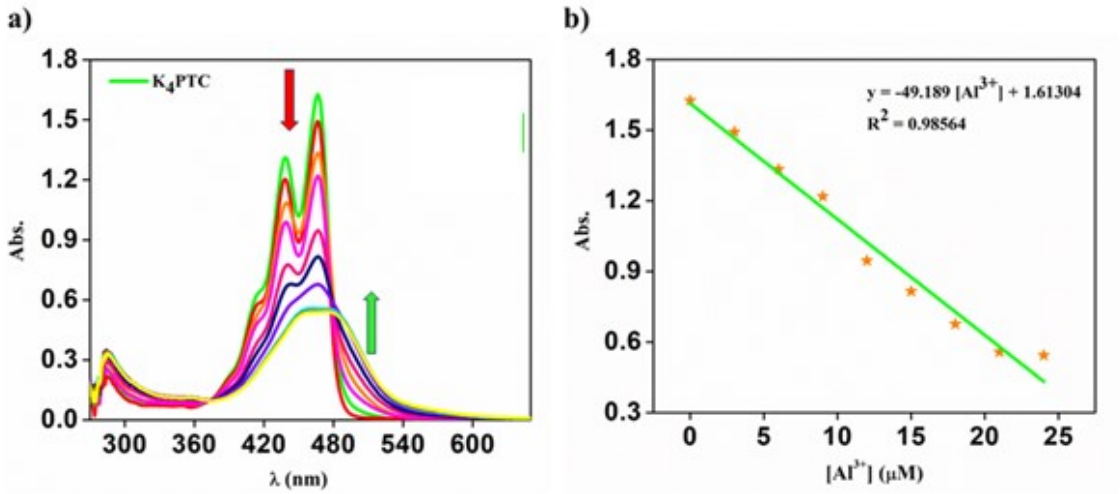

Figure S10: a) UV-Vis absorption spectra of K_4PTC solution in water upon addition of increasing concentration of Al^{3+} (aq) ion; b) Change in absorbance of the peak at 465 nm upon incremental addition of Al^{3+} ion.

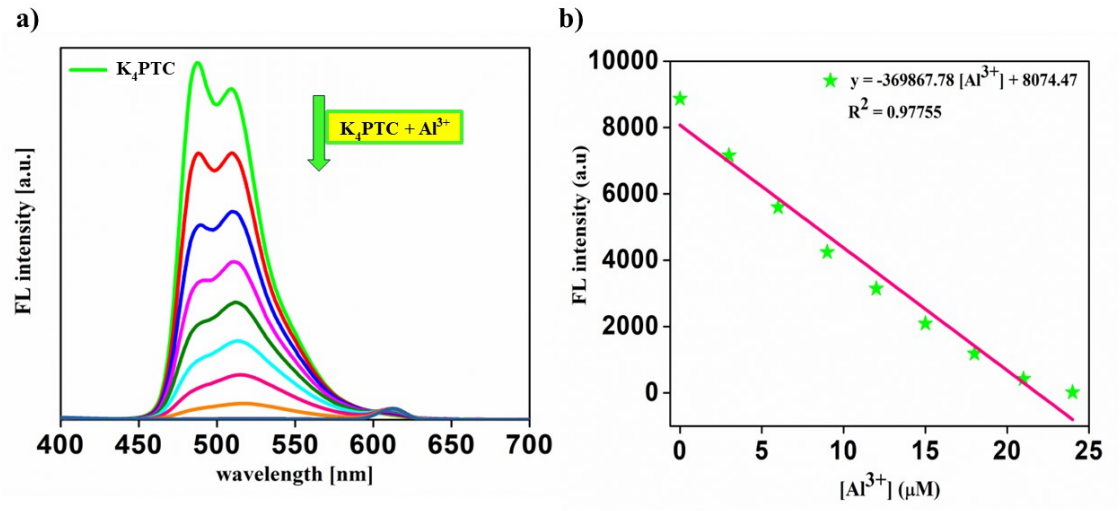

Figure S11: a) Emission spectra of K_4PTC solution in water upon addition of increasing concentration of Al^{3+} (aq); b) Change in emission intensity of the peak at 510 nm upon incremental addition of Al^{3+} ion.

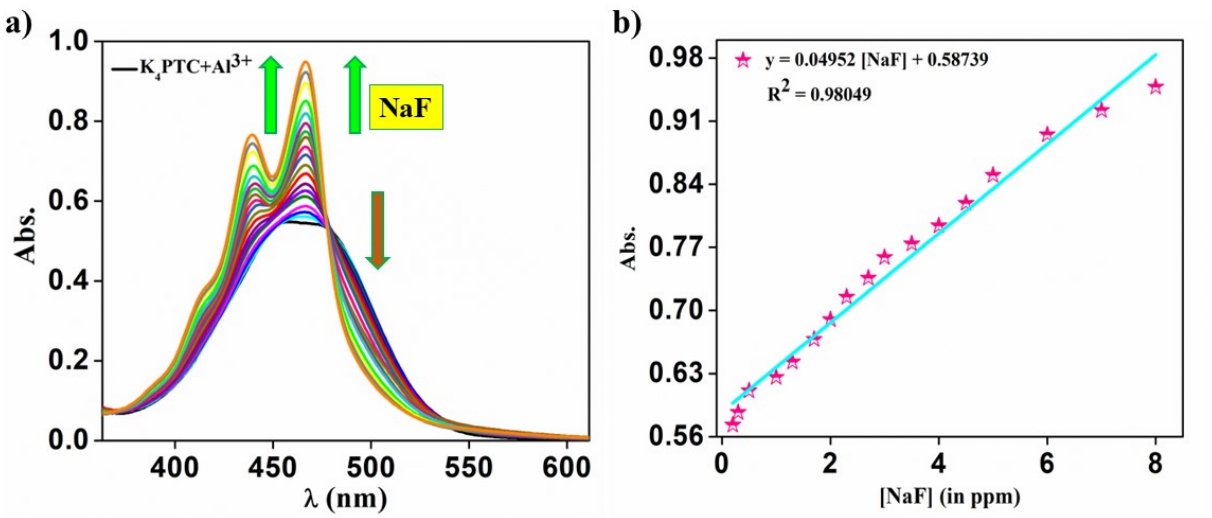

Figure S12: a) UV-Vis spectra of (K_4PTC + Al^{3+}) solution in water upon addition of increasing concentration of NaF (0-8 ppm) in water; b) Change in absorbance of the peak at 465 nm upon incremental addition of F^- ion

.

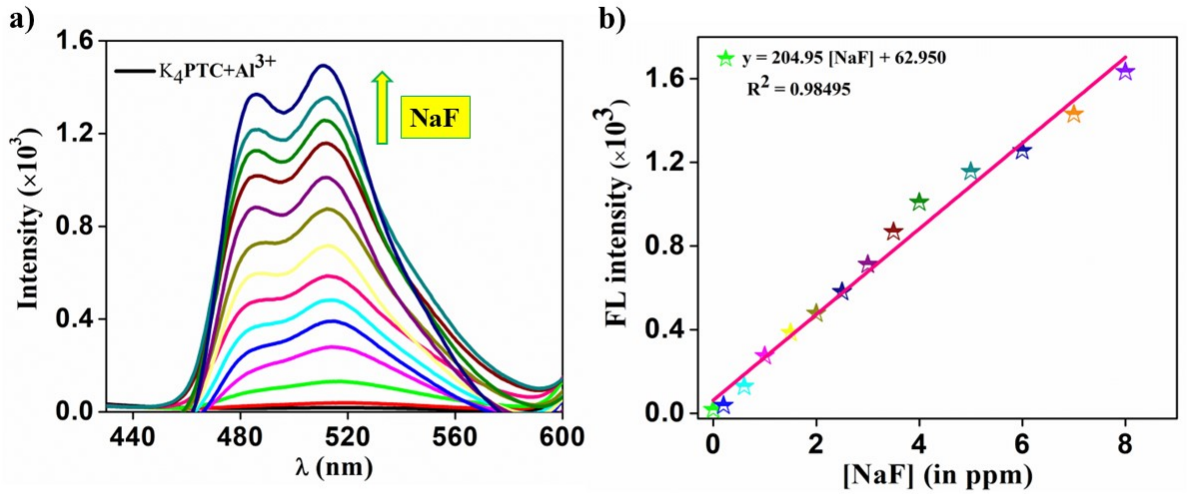

Figure S13: a) Fluorescence spectra of (K_4PTC + Al^{3+}) solution in water upon addition of increasing concentration of NaF (0-8 ppm) in water; b) Change in emission intensity of the peak at 510 nm upon incremental addition of F^- ion.

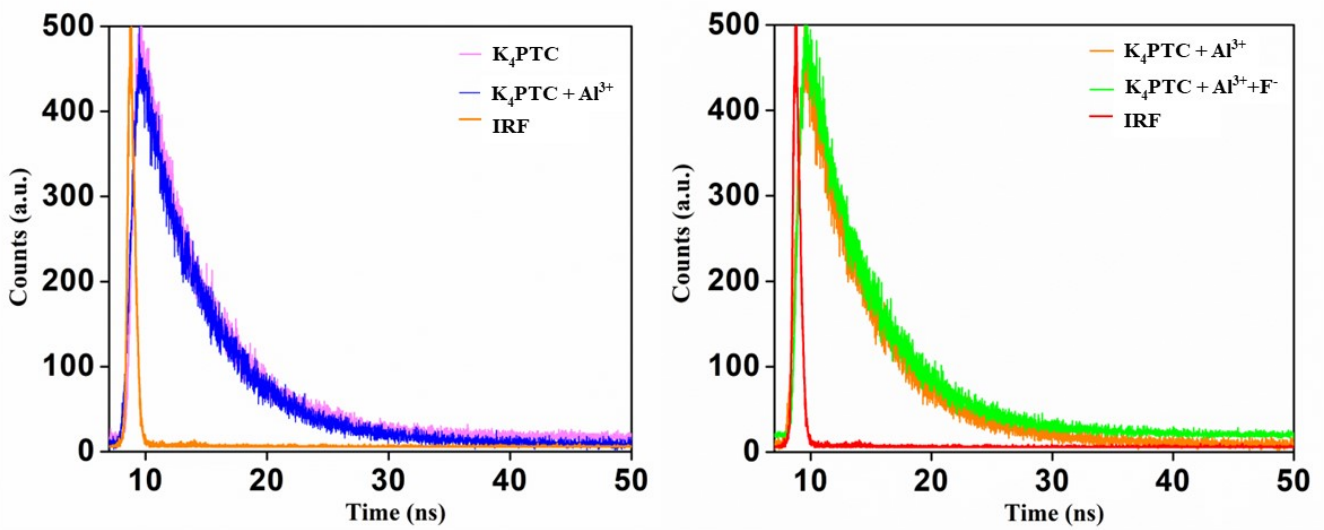

Figure S14: Time Resolved Photoluminescence study of **K_4PTC** solution in water and upon stepwise addition of Al^{3+} and F^-.

Observed	K_4PTC	K_4PTC(aq)	K_4PTC(aq)

Properties	(aq)	+ Al^{3+}(aq)	+ Al^{3+}(aq)+NaF(aq)
Quantum Yield (%)	81	9.2	74
Average life time (ns)	5.20	5.42	5.31
Radiative recombination rate (k_r) (s^{-1})	0.16×10^9	0.16×10^7	0.14×10^9
Non-radiative recombination rate (k_{nr}) (s^{-1})	8.7×10^7	0.17×10^9	4.9×10^7

Table S2: Quantum yield and the recombination rate of the **K_4PTC** solution upon addition of Al^{3+} and F^- ion.

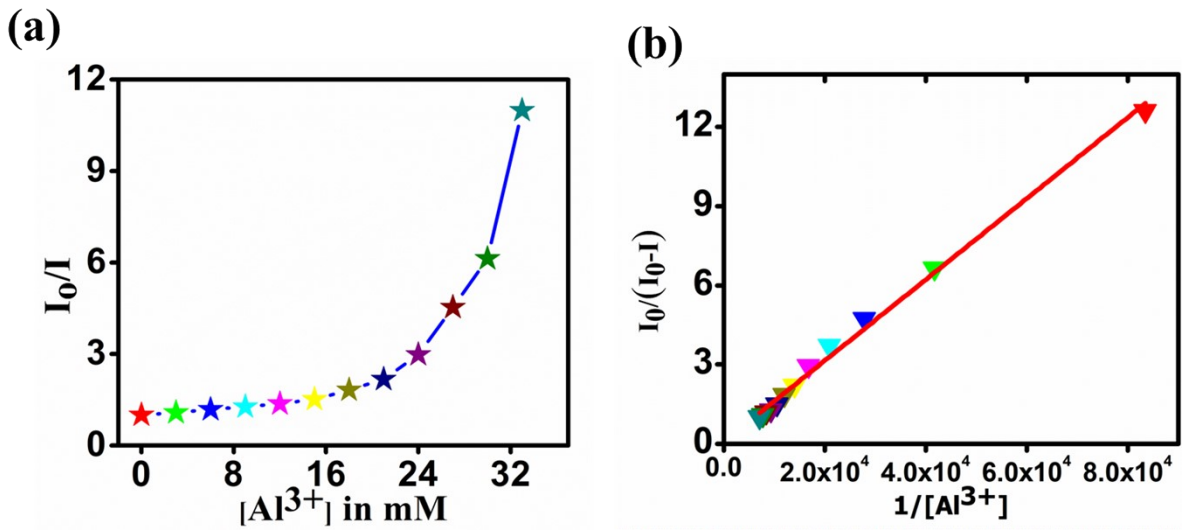

Figure S15: (a) Stern-Volmer plot for quenching of the fluorescence of **K_4PTC** upon addition of increasing concentration of Al^{3+}; (b) Benesi Hildebrand plot for the calculation of association constant for the association of Al^{3+} with **K_4PTC** in water (association constant $=6 \times 10^4$ M^{-1}).

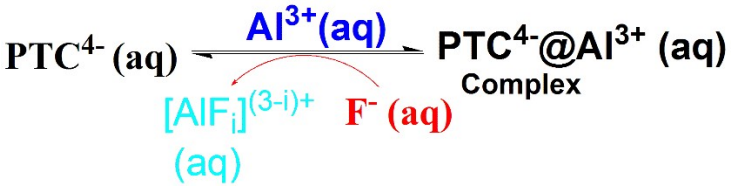

Figure S16: Plausible reactions involved in the sensing process

Real life sample analysis:

The methodology was validated by quantifying the fluoride ion concentration in real samples collected from Dengaon village, located in the Karbi Anglong district of Assam, India.

For the UV-Vis analysis, 2.5 mL of a 1.6 × 10^{-4} M solution of K_4PTC was placed in a cuvette, and 70 µL of a 10 × 10^{-3} M $AlCl_3$ solution in an aqueous medium was added. Subsequently, 50 µL of each water sample was added separately to each mixture. The resultant colorimetric response was analyzed using a UV-Vis spectrometer, and the absorbance at a wavelength of 465 nm was measured. The data was then compared with the calibration plot to determine the concentration of fluoride ions in the water samples. Similarly, the fluorescence detection was performed by monitoring the fluorescence intensity of the solution at 510 nm by exciting at 465 nm. For fluorescence measurement, 2.5 mL of 1.6 × 10^{-5} M solution of K_4PTC was placed in a cuvette, and 70 µL of a 1 × 10^{-3} M $AlCl_3$ solution in an aqueous medium was added. Then, 50 µL of each water sample was added separately to each mixture. The data was then compared with the calibration plot to determine the concentration of fluoride ions in the water samples. The results obtained corroborated the data from the fluoride ion-selective electrode.

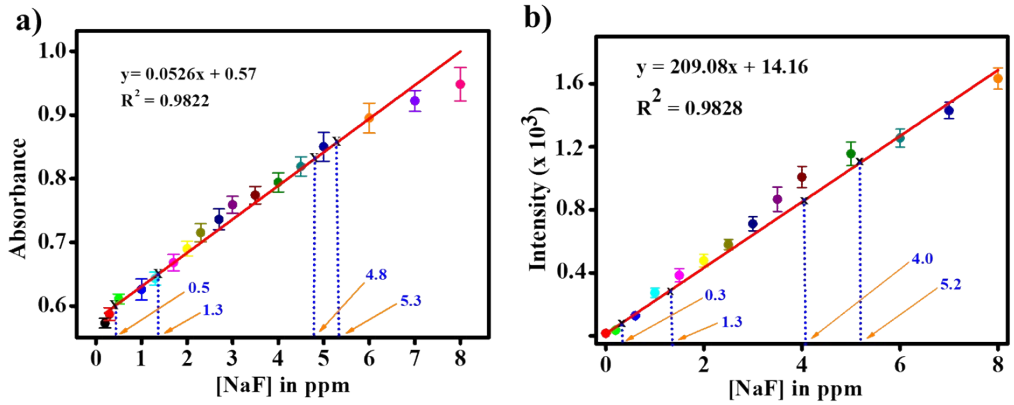

Figure S17: Concentration of fluoride ion in the water sample as per the calibration curve obtained by following the methodology demonstrated in this work a) UV-Vis spectroscopy; b) Fluorescence spectroscopy.

No.of Samples	Concentration (UV-Vis observation)	Concentration (FL observation)	Ion Selective Electrode	Error from UV-Vis observation	Error from FL observation
Sample 1	0.5 ppm	0.3 ppm		+0.22	+0.02
Sample 2	1.3 ppm	1.3ppm		+0.1	+0.1
Sample 2	4.8 ppm	4.0 ppm		+0.7	+0.1
Sample 3	5.3 ppm	5.2 ppm	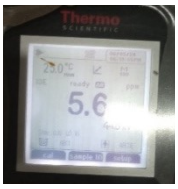	-0.3	-0.4

Table S3: Comparison between the two spectroscopic methods of measuring the concentration of F^- ion in water sample with fluoride ion selective electrode method.

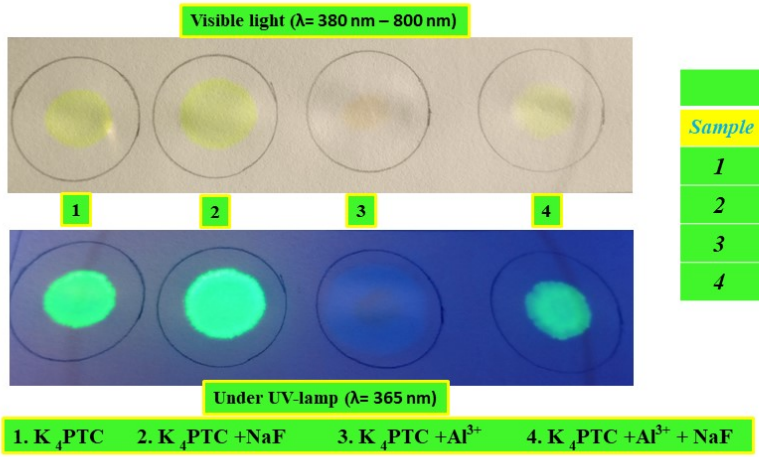

RGB Values			
Sample	*R*	*G*	*B*
1	*162*	*163*	*95*
2	*166*	*167*	*97*
3	*177.7*	*158.7*	*128.7*
4	*160.7*	*156.7*	*109.7*

Figure S18: Left: Visualization of the methodology in Paper strip, colorimetric and fluorescence changes of **K_4PTC** upon addition of aqueous solution of NaF and Al^{3+} under normal light and UV-Vis light, Right: RGB value of the colorimetric change.

Table S4: Comparison with some of the reported methods

Sl No.	MOF	Fluoride Salt used	Solvent used for study	LOD	Reference
1	Selective, Fast-Response, and Regenerable Metal−Organic Framework for Sampling Excess Fluoride Levels in Drinking Water	NaF	THF/Water	0.1 ppm	Ebrahim, F. M.; Nguyen, T. N.; Shyshkanov, S.; Gładysiak, A.; Favre, P.; Zacharia, A.; Stylianou, K. C. Selective, fast-response, and regenerable metal–organic framework for sampling excess fluoride levels in drinking water. *Journal of the American Chemical Society*, **2019**, *141*(7), 3052-3058.
2	Highly Sensitive Optical Sensor for Selective Detection of Fluoride Level in Drinking Water: Methodology to Fabrication of Prototype Device	NaF	Ethanol /Water	0.1 ppm	Chatterjee, A.; Pan, N.; Maji, T. K.; Pasha, S. S.; Singh, S.; Ahmed, S. A.; Pal, S. K. Highly sensitive optical sensor for selective detection of fluoride level in drinking water: methodology to fabrication of prototype device. *ACS Sustainable Chemistry & Engineering*, **2021**, *9*(20), 7160-7170.
3	Off/On Amino-Functionalized Polyhedral Oligomeric Silsesquioxane−Perylene Diimides Based Hydrophilic Luminescent	NaF	DMSO/ Water	16.2 ppb	Sun, M.; Liu, H.; Su, Y.; Yang, W.; Lv, Y. Off/on amino-functionalized polyhedral oligomeric silsesquioxane–

	Polymer for Aqueous Fluoride Ion Detection				perylene diimides based hydrophilic luminescent polymer for aqueous fluoride ion detection. *Analytical chemistry*, **2020,** *92*(7), 5294-5301.
4	Near-Infrared Fluoride Sensing Nano-Optodes and Distance-Based Hydrogels Containing Aluminum-Phthalocyanine	TBAF	THF (gel system at differen t pH)	0.1μM	Wang, L.; Zhang, Y.; Wang, L.; Cheng, Y.; Yuan, D., Zhai, J.; Xie, X. Near-Infrared Fluoride Sensing Nano-Optodes and Distance-Based Hydrogels Containing Aluminum-Phthalocyanine. *ACS sensors*, **2023**, *8*(11), 4384-4390.
5	Mixed lanthanide–organic frameworks with borono groups for colorimetric detection of excess fluoride levels in rivers	NaF	Suspen ded MOF solution in Water	0.16ppm at 544 nm and 0.84 ppm at 616 nm.	Cheng, P.; Min, H.; Zhu, Z.; Huang, M.; Zhou, J.; Zhao, N. Mixed lanthanide-organic frameworks with borono group for colorimetric detection of excess fluoride levels in river. *Inorganic Chemistry Frontiers*, **2024**.
6	Perylenemonoimide-Based Colorimetric Probe with High Contrast for Naked-Eye Detection of Fluoride Ions	TBAF	THF	0.495μM	Mu, M.; Ke, X.; Cheng, W.; Li, J.; Ji, C.; Yin, M. Perylenemonoimide-based colorimetric probe with high contrast for naked-eye detection of fluoride ions. *Analytical Chemistry*, **2022**, *94*(33), 11470-11475.
7	Selective and Fast Detection of Fluoride-Contaminated Water Based on a Novel Salen-Co-MOF Chemosensor	TBAF	DMSO/ H_2O	0.24μM	Alhaddad, M.; El-Sheikh, S. M. Selective and fast detection of fluoride-contaminated water based on a novel Salen-Co-MOF

					Chemosensor. *ACS omega*, **2021**, *6*(23), 15182-15191.
8	**This work:** Perylene Tetracarboxylate Dye Based Colorimetric and Fluorometric Sensor for ppb-Level Fluoride Detection in Water	NaF	Water	1 ppb (fluorometric); 0.2 ppm (colorimetric)	